Commissioning of a Multiple-Frequency–Modulation Smoothing by Spectral Dispersion Demonstration System on OMEGA EP

Introduction

Smoothing by spectral dispersion (SSD) has become a critically important method for smoothing laser-imprinted nonuniformities in target implosions.[1] The spot shape on target is generally controlled using distributed phase plates (DPP's), which effectively control the low-order beam profile but introduce fine-scale speckle structures that require smoothing.[2] Recently, a new concept for a one-dimensional (1-D) SSD system was proposed that utilizes multiple frequencies for phase modulation (multi-FM SSD).[3] By carefully selecting modulation frequencies, resonant features that often limit the effectiveness of SSD systems can be eliminated. As a result, effective beam smoothing can be achieved with a 1-D system using a modest modulation bandwidth in a frequency-conversion scheme that utilizes a single tripler crystal. These features allow for the integration of multi-FM SSD into either the OMEGA EP Laser System[4] or the National Ignition Facility (NIF)[5] laser.

Polar-drive experiments on the NIF will require pulse shapes that incorporate multi-FM SSD.[6] Conceptual pulse shapes are illustrated in Fig. 134.1. The three different shapes correspond to three different latitudes of the beams entering the NIF target chamber, with Ring 1 corresponding to higher latitudes and Ring 3 being nearest the equator. Beam smoothing using multi-FM SSD is required only during the three pickets at the beginning of the pulse. During the main pulse, at which higher power levels are required and amplitude modulation becomes a correspondingly greater concern, only the standard NIF 1-D SSD and stimulated Brillouin scattering suppression (SBSS) would be applied. Therefore, dynamic application of the multi-FM SSD bandwidth must be accommodated in the system design.

To demonstrate multi-FM SSD on a laser system with an architecture similar to the NIF, a prototype system was developed and integrated into a long-pulse beamline of OMEGA EP. Simulations of amplitude modulation caused by free-space propagation of a frequency-modulated beam in the OMEGA EP beamline and the design and performance of the fiber front end supporting multi-FM experiments on OMEGA EP are

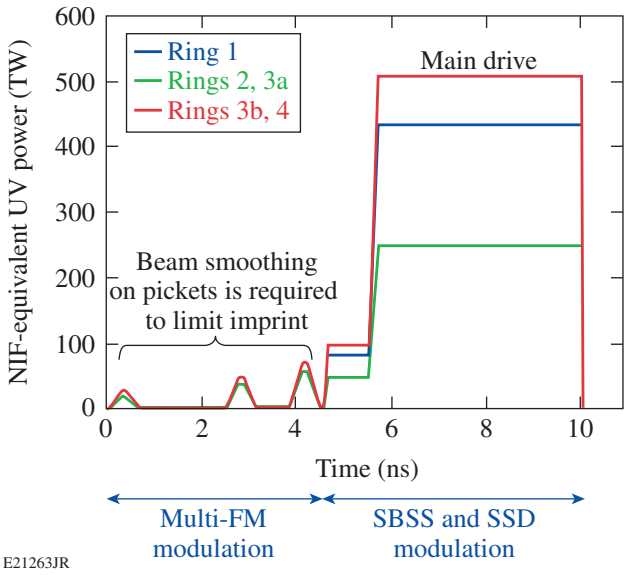

Figure 134.1
Representative triple-picket pulse shapes for polar-drive experiments on the NIF. The three pulse shapes correspond to beams entering the target chamber at different latitudes. In all cases, multi-FM smoothing by spectral dispersion (multi-FM SSD) is applied for only the picket pulses. SBSS: stimulated Brillouin scattering suppression.

presented in ***Simulations of the Propagation of Multiple-FM Smoothing by Spectral Dispersion on OMEGA EP*** (p. 85) and ***Fiber Front End with Multiple Phase Modulations and High-Bandwidth Pulse Shaping*** (p. 98). This article describes the prototype system and presents results from the integration and commissioning on the OMEGA EP beamline. Particular attention is paid to the important issue of amplitude modulation in the high-power beam at critical points in the system.

System Description

The prototype multi-FM SSD front end is illustrated in Fig. 134.2. A fiber front end comprises two separate channels—a main-pulse channel and a multi-FM picket channel.[7] (Details on the phase modulation for multi-FM and other system specifications can be found in Table 134.I.) The main-pulse channel is similar to the NIF front end, including phase modulation at 3 GHz for SBSS and 17 GHz for SSD, although the

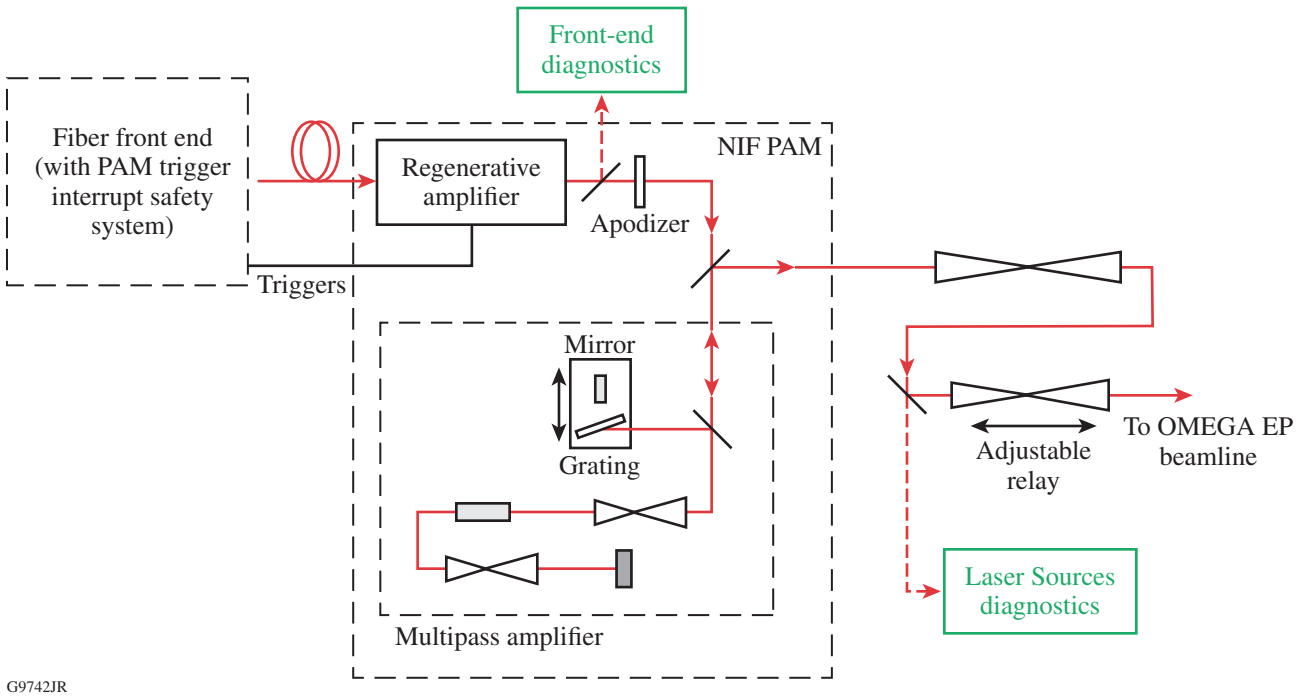

Figure 134.2
Schematic layout of the multi-FM SSD prototype front end. Red lines indicate the optical path, black lines indicate electrical trigger signals, and green blocks indicate laser diagnostics. PAM: preamplifier module.

Table 134.I: Specifications of the multi-FM SSD demonstration system.

Parameter	Value
Modulation frequencies (f_1, f_2, f_3)	21.165, 22.837, 31.881 GHz
Modulation indices (δ_1, δ_2, δ_3)	0.45, 1.04, 2.07 rad
Grating angular dispersion (in PAM), $d\theta/d\lambda$	381.4 μrad/Å
Spectral bandwidth	7.3 Å
Magnification, PAM to beamline	21.5
Temporal skew from pulse-front tilt	229 ps

17-GHz, 1-D SSD phase modulation was not utilized for high-energy shots.

The two channels are fiber optically combined and injected into a NIF preamplifier module (NIF PAM).[8] Pulses are initially amplified to the mJ level in a regenerative amplifier. The fiber front end also contains a system safety feature called the PAM trigger interrupt safety system (PTISS), which monitors the seed pulses and prevents emission of an amplified pulse from the regenerative amplifier in the event of an unsafe condition.[7] Upon exiting the regenerative amplifier, the beam is passed through an apodizer that shapes the edges of the beam and precompensates for spatial-gain variations in the beamline amplifiers. After an image relay, the beam is injected into a multipass amplifier (MPA), where it undergoes amplification to ~500 mJ via four passes through a flash-lamp–pumped, 32-mm-diam × 300-mm-long Nd:glass rod amplifier. The beam is angularly multiplexed in the MPA and passes through a spatial filter with an array of four 5.16-mm-diam pinholes on each pass. After accounting for magnification into the OMEGA EP beamline, these pinhole sizes correspond to a full-angle acceptance of ~200 μrad in the final OMEGA EP beam, making them the tightest pinholes in the system.

A diffraction grating inserted into the MPA after the second pass of the MPA disperses the SSD bandwidth. The 1700-lines/mm gold grating is aligned at the Littrow angle and mounted on a translation stage that also supports a flat mirror. This allows us to translate the mirror into place and operate the system without any angular dispersion of the SSD bandwidth. Note that because phase modulation is performed in a fiber system, there is no pre-shear diffraction grating as found

in most SSD systems. As a result, the dispersing diffraction grating also introduces a pulse-front tilt, or temporal shear, of 229 ps across the beam width.

After exiting the NIF PAM, the beam passes through a set of image relays and is injected into the OMEGA EP beamline. One of the image relays is adjustable to allow for fine control of the image plane's position.

Two sets of beam diagnostics are provided within the multi-FM front-end system. The front-end diagnostics characterize the output of the regenerative amplifier and comprise an energy diagnostic, a spectrometer (<5-GHz resolution), and fast photodetection (45-GHz response) for measuring amplitude noise. The Laser Sources diagnostics, characterizing the beam at the output of the NIF PAM, contain energy diagnostics, cameras that image the near-field and far-field beam profiles, a streak camera that measures the pulse shape, and a setup for measuring the amplitude noise near an image plane of the diffraction grating.

The pulse exiting the Laser Sources Bay is injected into the OMEGA EP long-pulse beamline (illustrated in Fig. 134.3). The OMEGA EP beamline is similar to a folded version of the NIF beamline. The beamline is an angularly multiplexed system in which a pulse undergoes two passes through the seven-disk booster amplifier and four passes through the eleven-disk main amplifier. The transport and cavity spatial filters (TSF and CSF, respectively) are each populated with 300-μrad full-angle pinholes to filter high-frequency spatial modulations on the beam. After undergoing full amplification in the beamline, the pulse exits the TSF and propagates to the frequency-conversion crystals (FCC's), which convert the 1.053-μm beam to the third harmonic. One critical difference from the NIF system is that the FCC's are physically separated from the final focusing optics by 8 m. The final focusing optics include a DPP, a focusing lens (f = 3.4 m), a vacuum window, and a thin debris shield.

Finally, one important consideration for a frequency-converted system with SSD is that the 1ω beam at the input of the frequency conversion should have a minimal amplitude modulation (AM). Because propagation away from the dispersing grating in a SSD system will convert FM to AM, it is beneficial to accurately image the grating to the FCC plane. This was accomplished on OMEGA EP by translating the

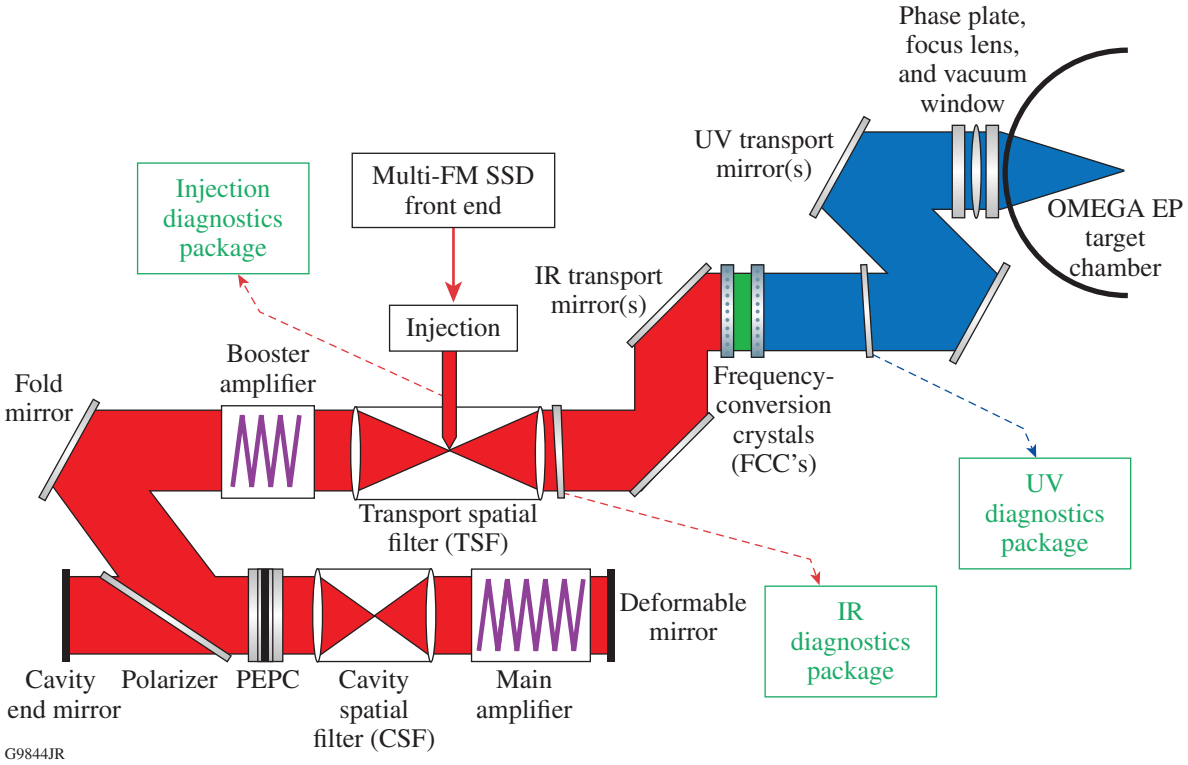

Figure 134.3
Schematic layout of the OMEGA EP long-pulse beamline. PEPC: plasma-electrode Pockels cell.

adjustable image relay in the front end (see Fig. 134.2) to shift the grating image plane onto the FCC's.

Three different diagnostics packages monitor the beam properties at various points in the system. An injection diagnostic package measures the energy, pulse shape, and near-field beam profile of the beam prior to up-collimation into the beamline. At the output of the beamline, the infrared diagnostics package (IRDP) contains diagnostics that measure the energy, near-field and far-field beam profiles, pulse shape, and wavefront of the 1ω amplified beam. Finally, after the frequency conversion, the ultraviolet diagnostics package (UVDP) measures the energy in the first, second, and third harmonics, and the near field, far field, and pulse shape of the 3ω beam. The UVDP also has provisions for inserting a DPP to measure the focal spot at an equivalent target plane.

Amplitude-Modulation Concerns

One of the key concerns with frequency modulation in a high-energy laser system is the generation of high peak intensities caused by AM. FM can be converted into AM by a number of mechanisms.[9] Ideally, a direct AM measurement in the planes of all the optics would ensure that AM is within tolerable levels; however, this measurement would be extremely difficult to make. A streak camera—the deployed pulse-shape diagnostic—does not have sufficient resolution to accurately measure noise at the multi-FM SSD frequencies. Therefore, for this demonstration, our approach was to measure the AM in the front end of the system and produce a budget for further AM in the beamline, based on simulations where possible and on conservative estimates where simulation was impossible. This budgeting process, which resulted in a limit to the peak power that could be safely produced on the system, is described in this section along with the results.

1. Amplitude Modulation in the UV Optics

A model of multi-FM propagation in the final stages of the OMEGA EP system is presented in ***Simulations of the Propagation of Multiple-FM Smoothing by Spectral Dispersion on OMEGA EP*** (p. 85).[10] The model, implemented in the laser simulation code Miró,[11] simulated a pulse with multi-FM SSD, beginning from the final pinhole in the TSF and propagating to the final UV optics at the target-chamber port. The pulse was assumed to be free of AM and to cleanly propagate through this final pinhole, and the SSD diffraction grating was assumed to be well imaged to the FCC plane. Amplitude modulation caused by the frequency-conversion process and propagation away from the FCC's was simulated, and a spatiotemporal model of the pulse intensity was developed for each optic. From this data, the *B*-integral (ΣB) accumulated from the final pinhole through the remaining transmissive optics was calculated. To keep the accumulated ΣB below 2.0 rad, it was determined that the maximum 3ω power on target (in the absence of other sources of AM) should be limited to 1.6 TW. Note that the simulations were performed assuming a grating with a larger dispersion (1800 lines/mm) than was actually used for this commissioning. Using this result as a basis for setting a system performance limit was therefore a conservative approach.

2. Amplitude Modulation via Amplification in the OMEGA EP Beamline

Amplification of the broadband multi-FM pulse can lead to FM-to-AM conversion and therefore must be considered when apportioning a budget for AM in the laser chain. Specifically, we consider the effects of material dispersion, gain narrowing, and phase changes caused by the line shape of the gain medium, referred to as the Kramers–Kronig phase. Additional effects such as etaloning in the system's optics or spectral clipping on the pinholes were not considered because these effects are specific to the optics and alignment of the particular beamline. A broadband, 1-D model of the IR portion of OMEGA EP, including material dispersion of all of the optics, the gain spectrum of the Nd-doped, LHG-8 glass amplifiers, and the phase introduced by this gain spectrum, was developed. Because the multi-FM spectral width is comparable to that of the gain spectrum of the Nd:glass, one expects that gain narrowing and the associated phase effects may alter both the power spectrum and the spectral phase of the multi-FM pulse, thereby producing AM.

Figure 134.4 shows the results of the model described above for a noise-free multi-FM pulse that is injected into the beamline (red). The multi-FM spectrum was created using the parameters shown in Table 134.I. This simulation shows that one can expect some FM-to-AM conversion to take place in the amplifier chain, producing an output pulse with amplitude modulation (blue). Zooming in on the modulation pattern, it is clear that amplification of the FM pulse in the OMEGA EP laser chain will lead to about a 10% peak-to-mean modulation on the pulse as a result of the effects considered in the model. This amount of AM must be included in the modulation budget as will be discussed in the following section.

3. Peak-Power Specification and AM Budget

A budget to allow for a reasonable level of AM accumulation in the OMEGA EP Laser System was developed to specify a peak power. The 1.6 TW determined from the Miró model of the final optics was used as a starting point, and allowances

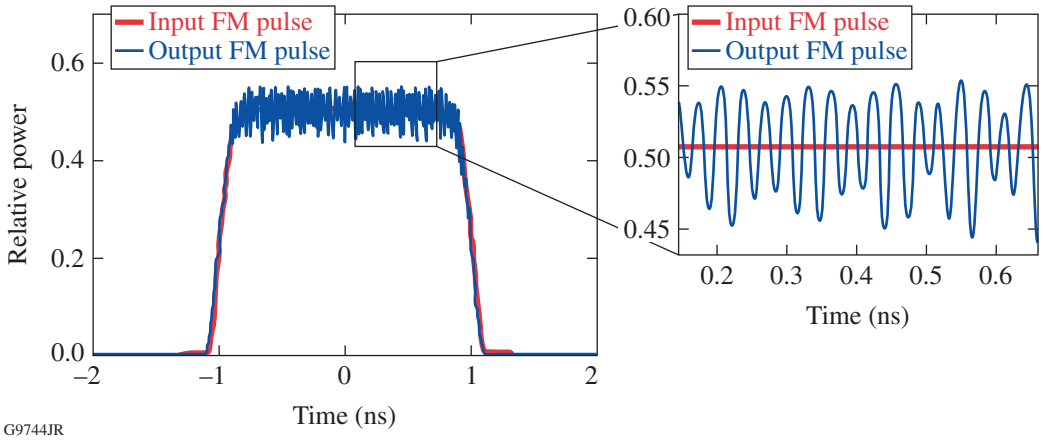

Figure 134.4
Result of a simulation of amplitude modulation in a 1ω pulse introduced by amplification in the OMEGA EP beamline.

were made for other sources of AM. The first of these was AM arising in the beamline (via dispersion, gain narrowing, and the Kramers–Kronig phase), as discussed in **Amplitude Modulation via Amplification in the OMEGA EP Beamline** (p. 78). The second was AM arising from "technical" sources of AM that cannot be predicted via simulation. These include AM arising from etalons, loss of spectrum from clipping on pinholes, etc. Finally, an allowance was made for residual AM in the front end. These sources of AM were assumed to contribute incoherently and were root sum squared to form an overall budget. Finally, a safety margin was applied to allow for both model uncertainties and energy instability in the system. A summary of the AM budget is shown in Table 134.II.

The result of the budgeting process is that the maximum UV on-target power for which OMEGA EP will utilize the multi-FM SSD system is 0.85 TW.

System Integration and Commissioning

1. Spectral Dispersion Concerns in the PAM Spatial Filters

One of the key concerns in limiting AM in the SSD system is to ensure that the spectrum, which is dispersed in the far field as a result of dispersion from the diffraction grating, cleanly passes through the pinholes of the system. The limiting pinholes in the system are in the multipass amplifier in the NIF PAM, i.e., the first pinholes after the diffraction grating. Therefore, the dispersion of the grating was selected to ensure that the beam can propagate through these pinholes without spectral clipping. To evaluate this, the far-field camera in the Laser Sources diagnostics (see Fig. 134.2) was used to image the dispersed spectrum at the output of the PAM and compared to the expected spectrum resulting from the multi-FM modulation. The result is shown in Fig. 134.5.

Inspection of the plot in Fig. 134.5(b) clearly shows that all the significant sidebands of the modulation spectrum can be observed in the output beam and therefore are not being clipped in the pinholes. In fact, under perfect alignment conditions, the pinhole cutoff frequency is given by

$$f_{\text{cutoff}} = \frac{c}{\lambda_0^2} \frac{\theta_{1/2}}{(\mathrm{d}\theta/\mathrm{d}\lambda)_{\text{grating}}}, \tag{1}$$

Table 134.II: Amplitude modulation budget and peak-power specification.

	Allowance	Resulting Peak Power
B-integral in UV optics (Miró model)	—	1.6 TW
AM in front end	15% peak to mean	—
AM introduced in beamline	10% peak to mean	—
Other "technical" sources of AM	20% peak to mean	—
Root-sum-square total	27%	1.17 TW
Safety margin	28%	**0.85 TW**

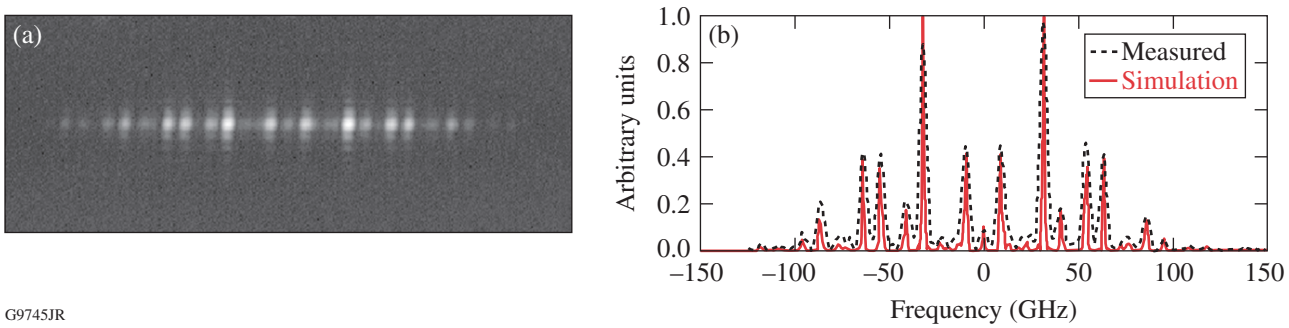

Figure 134.5
(a) Far-field image of the beam exiting the PAM with multi-FM SSD applied. (b) Lineout of the far-field image (black dashed line) with the calculated modulation spectrum superimposed (red solid line), with the far-field camera spatial scale converted to the spectral domain based on the grating dispersion and the magnification to the camera.

where $\theta_{1/2}$ is the acceptance half-angle of the spatial filter (2.07 mrad for the spatial filter with a 1.249-m-focal-length lens and 2.58-mm-radius pinhole), $(d\theta/d\lambda)_{grating}$ is the angular dispersion of the diffraction grating (given in Table 134.I), and λ_0 is the central frequency of the seed source (1053.044 nm). The result is an ideal cutoff frequency of 146 GHz, significantly higher than the highest signal frequency shown in Fig. 134.5. In practice, the pinhole cutoff will be somewhat lower because of misalignment into the spatial filters and between the multiple passes through the MPA. Finally, noise measurements on the beam at the output of the MPA in the Laser Sources diagnostics have confirmed that the AM is below the 15% peak-to-mean allowance in Table 134.II (see Fig. 134.34).

2. Commissioning on OMEGA EP

The commissioning process on OMEGA EP proceeded by initially activating without dispersion of the modulation bandwidth, by removing the diffraction grating from the beam path in the NIF PAM and inserting the mirror (see Fig. 134.2). Each of the two channels (the multi-FM SSD channel and the main-pulse channel) was introduced individually. Initial shots were taken just within the Laser Sources Bay to confirm stability and acceptable beam quality and to develop configurations to produce the appropriate energies. Subsequent shots energy ramped the system first just to the beamline output. Finally, a UV energy ramp to the system limits was undertaken and the picket and main channels were combined. After full-system performance was demonstrated, the diffraction grating was inserted and the system was methodically ramped to full performance. Only the final results are presented herein.

Results from a UV shot near the 0.85-TW system limit using a triple-picket pulse applied to the multi-FM channel (no main pulse) are shown in Fig. 134.6: the near-field beam profiles at the injection [Fig. 134.6(a)]; beamline output [Fig. 134.6(b)]; and the UV output [Fig. 134.6(c)]. The beam quality as shown is comparable to a typical performance on this beamline with the narrowband OMEGA EP front end. The UV pulse shape, calibrated to on-target power [shown in Fig. 134.6(d)], indicates that the shot did, in fact, achieve a peak power of >0.8 TW.

The far-field intensities measured on a multi-FM picket-only shot are plotted in Fig. 134.7. The measured focal spot at the beamline output, from the far-field camera in the IRDP, is shown in Fig. 134.7(a). A lineout of this image along with the simulated dispersion of the modulation spectrum is shown in Fig. 134.7(b). The same measurements at 3ω from the UV far-field camera are shown in Figs. 134.7(c) and 134.7(d). Note that the wavefront error accumulated in the beamline has broadened these focal spots, making the different sidebands of the 1ω spectrum difficult to distinguish in the IR far-field image. The width of the focal-spot lineout is consistent, however, with the width of the simulated spectrum, providing evidence that the spectrum is not clipped by propagation in the beamline.

The 3ω spectrum is by design very complex with a large number of closely spaced sidebands approximating a quasi-uniform modulation spectrum. As a consequence, the far field approximates a continuously blurred version of the narrowband far-field profile, with the blurring applied in one dimension. Note in Fig. 134.7(d) that the width of the far field is consistent with the width of the modulation spectrum, indicating that the full spectrum was frequency converted.

In addition to the triple-picket pulse shape shown in Fig. 134.6(d), a variety of other pulse shapes have been used with the multi-FM SSD source in the process of commissioning. The sample shown in Fig. 134.8 includes a narrow

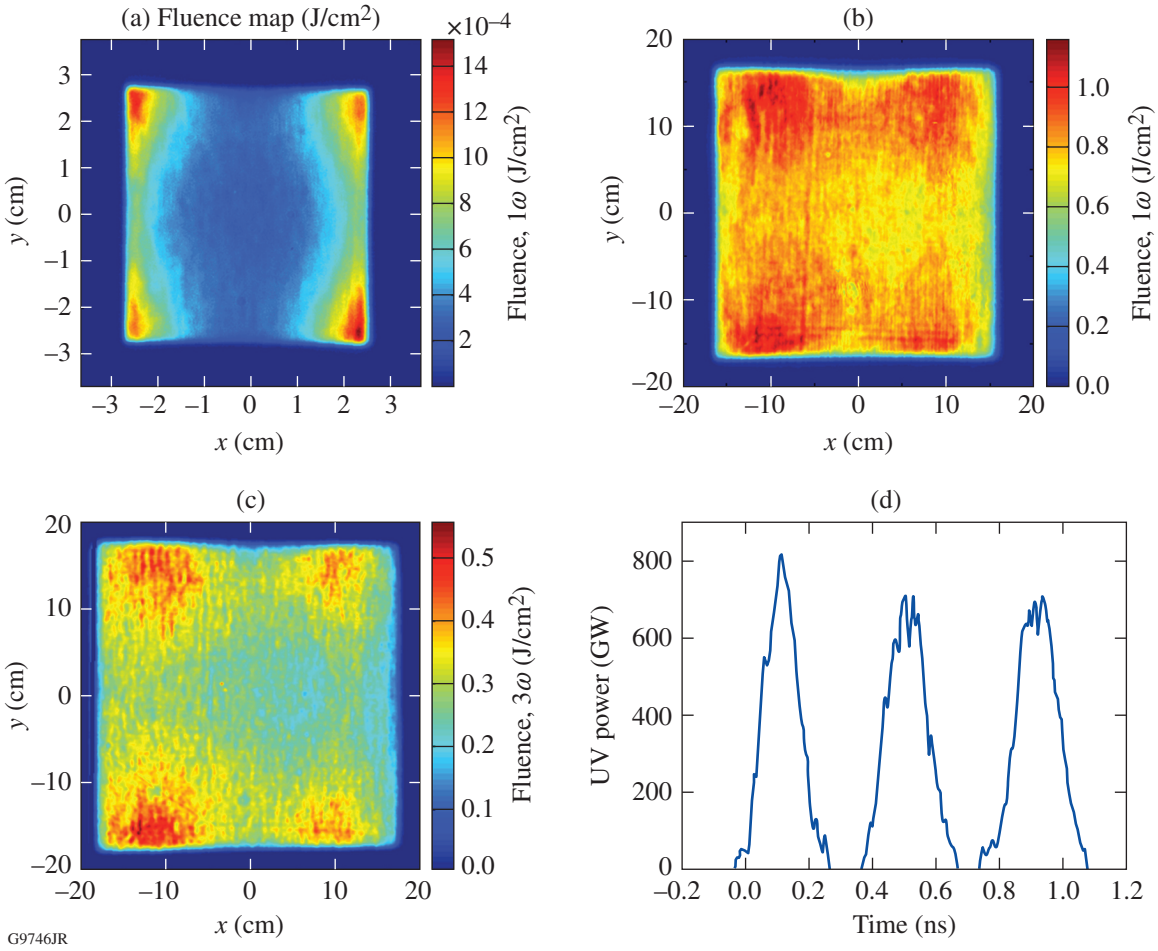

Figure 134.6
Beam profile at various points in the system for a triple-picket multi-FM SSD shot near the system performance limit. Beam profiles as measured by the near-field cameras in the (a) injection diagnostics, (b) IRDP, and (c) UVDP; (d) the UV pulse shape as measured by the streak camera in the UVDP.

150-ps picket [Fig. 134.8(a)], a series of three 650-ps pickets [Fig. 134.8(b)], and a 2-ns square pulse at the system power limit [Fig. 134.8(c)].

3. Demonstration of Beam-Smoothing Performance

Upon completion of the commissioning of the multi-FM SSD demonstration system on OMEGA EP, an experiment was performed to demonstrate the resulting beam smoothing. A DPP, designed to produce a super-Gaussian spot with a 1.1-mm diameter at the target plane, was mounted in the UV diagnostics path. In this configuration, the UV far-field camera measures the fluence distribution in an equivalent target plane. For this experiment, a single 650-ps picket pulse was used.

A baseline measurement was first made with the narrow-bandwidth main-pulse source (with only the 3-GHz SBSS bandwidth applied). To eliminate any dispersion of even this low bandwidth, the PAM diffraction grating was not used and was replaced with the mirror. The resulting target-plane intensity distribution is shown in Fig. 134.9(a). Lineouts through the center of the beam in both the horizontal and vertical directions [shown in Fig. 134.9(b)] indicate a high speckle contrast.

A smoothed beam profile was measured using the identical pulse shape formed with the multi-FM picket seed source. The diffraction grating was reinserted into the beam path in the PAM to provide dispersion of the bandwidth. The smoothed target-plane intensity distribution is plotted in Fig. 134.9(c) and the corresponding lineouts in Fig. 134.9(d). The effect of SSD on the beam profile is clear, with the smoothing being more effective in the horizontal (dispersion) direction, as expected in a 1-D SSD system.

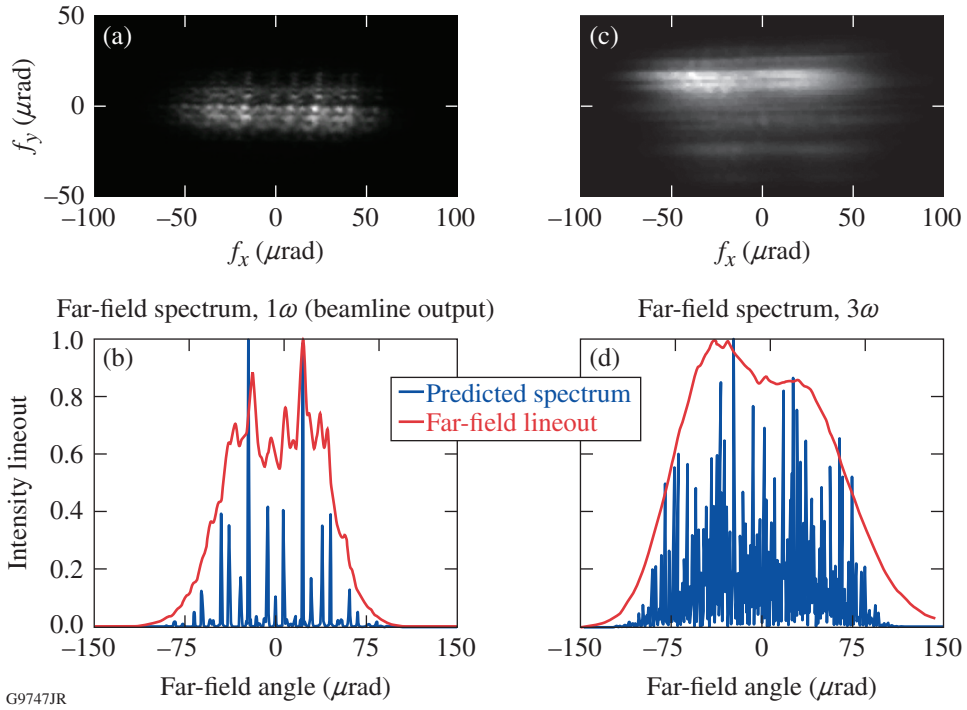

Figure 134.7
Far-field measurements at the [(a) and (b)] IRDP and [(c) and (d)] UVDP for a multi-FM picket shot. [(a) and (c)] The raw images are shown with the scale calibrated to the far-field angle in μrad. [(b) and (d)] The simulated optical spectra are plotted (in blue) along with lineouts from the camera images (red).

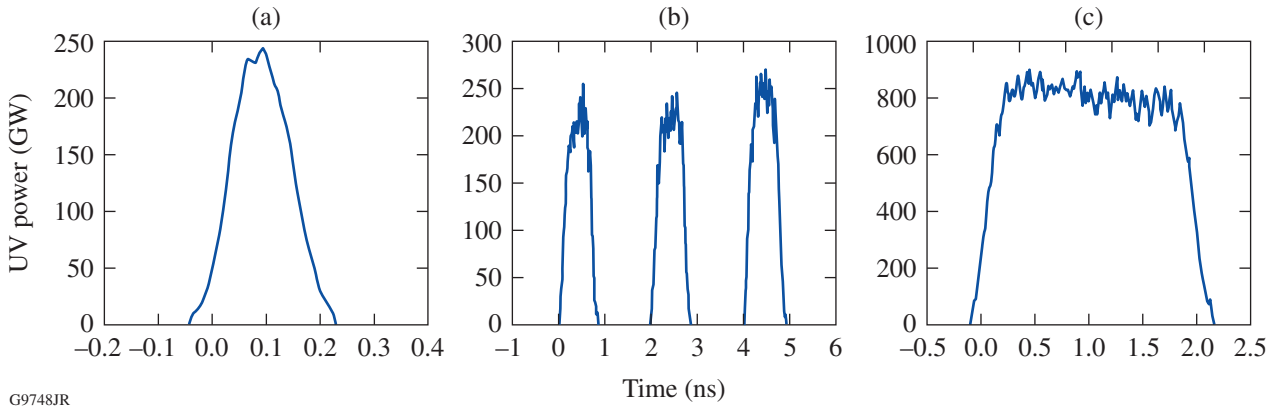

Figure 134.8
UV streak-camera measurements of a variety of multi-FM pulse shapes used during commissioning. (a) A single 150-ps full-width-at-half-maximum (FWHM) picket, (b) a sequence of three 650-ps FWHM pickets, and (c) a 2-ns square pulse.

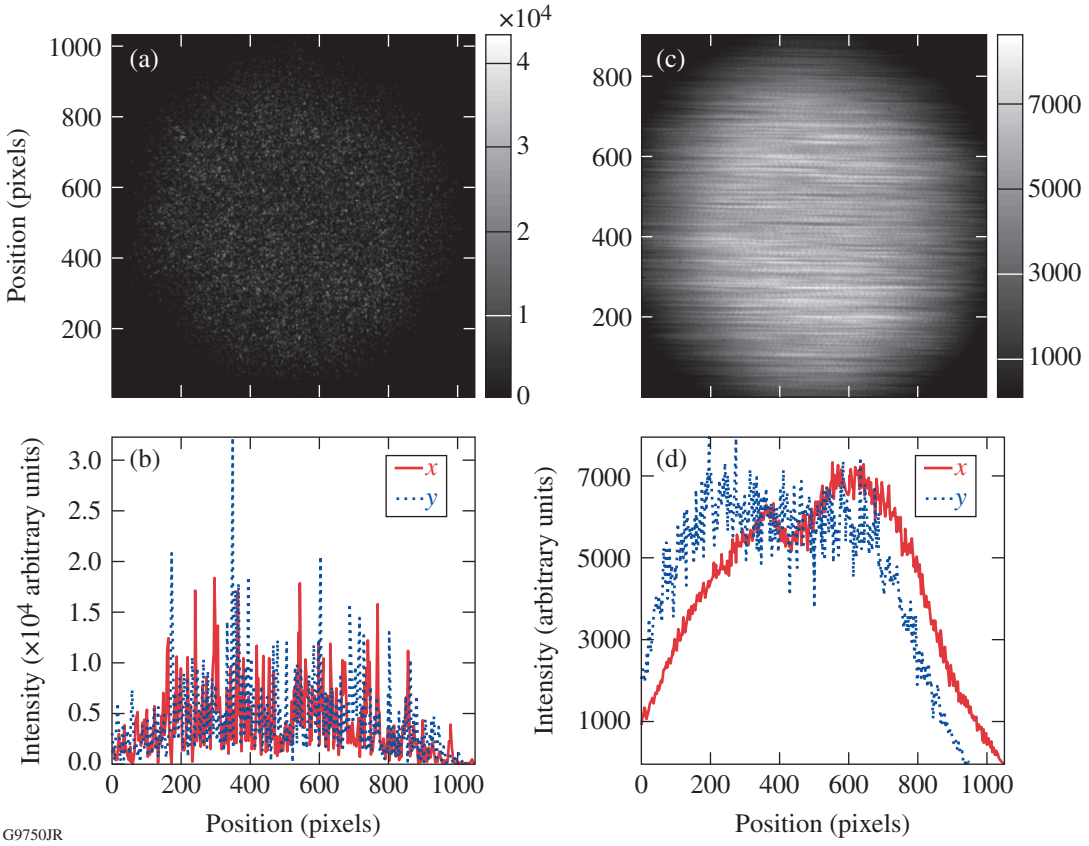

Figure 134.9
Equivalent-target-plane fluence measurements showing beam smoothing caused by multi-FM SSD applied to a 650-ps picket pulse. [(a) and (c)] Fluence profiles and [(b) and (d)] fluence lineouts in the horizontal and vertical directions are plotted for a narrowband main-channel pulse and a multi-FM SSD pulse, respectively.

Conclusion

A prototype multi-FM SSD demonstration system has been successfully commissioned on a long-pulse beamline of the OMEGA EP Laser System. The system utilizes a fiber-based front end with a NIF PAM to deliver dispersed, phase-modulated pulses to the beamline, where the beam is amplified, converted to the third harmonic, and focused on the target after a DPP. A 0.85-TW limit for the peak power delivered to the target using the multi-FM SSD system was derived from a combination of simulating pulsed beam propagation through the UV optics, modeling the beamline gain processes, and budgeting for other potential sources of amplitude modulation. The multi-FM system was operated up to the system power limit using a variety of pulse shapes, and no evidence of spectral loss or beam degradation was observed on the available diagnostics. The beam-smoothing improvement obtained with the multi-FM SSD system was characterized using equivalent-target-plane fluence-profile measurements.

Since commissioning on OMEGA EP, the multi-FM system has been used in a number of target campaigns with the goal of validating the predicted effect on target physics. This work is ongoing, and the system will continue to provide useful data critical to future OMEGA EP experiments and potentially future polar-drive fusion experiments.

ACKNOWLEDGMENT

This work was supported by the U.S. Department of Energy Office of Inertial Confinement Fusion under Cooperative Agreement No. DE-FC52-08NA28302, the University of Rochester, and the New York State Energy Research and Development Authority. The support of DOE does not constitute an endorsement by DOE of the views expressed in this article.

REFERENCES

1. S. Skupsky, R. W. Short, T. Kessler, R. S. Craxton, S. Letzring, and J. M. Soures, J. Appl. Phys. **66**, 3456 (1989).

2. Y. Kato *et al*., Phys. Rev. Lett. **53**, 1057 (1984).

3. *LLE Review Quarterly Report* **114**, 73, Laboratory for Laser Energetics, University of Rochester, Rochester, NY, LLE Document No. DOE/NA/28302-826, OSTI ID 93524 (2008).

4. J. H. Kelly, L. J. Waxer, V. Bagnoud, I. A. Begishev, J. Bromage, B. E. Kruschwitz, T. J. Kessler, S. J. Loucks, D. N. Maywar, R. L. McCrory, D. D. Meyerhofer, S. F. B. Morse, J. B. Oliver, A. L. Rigatti, A. W. Schmid, C. Stoeckl, S. Dalton, L. Folnsbee, M. J. Guardalben, R. Jungquist, J. Puth, M. J. Shoup III, D. Weiner, and J. D. Zuegel, J. Phys. IV France **133**, 75 (2006).

5. G. H. Miller, E. I. Moses, and C. R. Wuest, Opt. Eng. **43**, 2841 (2004).

6. T. J. B. Collins, J. A. Marozas, K. S. Anderson, R. Betti, R. S. Craxton, J. A. Delettrez, V. N. Goncharov, D. R. Harding, F. J. Marshall, R. L. McCrory, D. D. Meyerhofer, P. W. McKenty, P. B. Radha, A. Shvydky, S. Skupsky, and J. D. Zuegel, Phys. Plasmas **19**, 056308 (2012).

7. "Fiber Front End with Multiple Phase Modulations and High-Bandwidth Pulse Shaping," published in this volume.

8. M. Bowers *et al*., in *Solid State Lasers XVI: Technology and Devices*, edited by H. J. Hoffman, R. K. Shori, and N. Hodgson (SPIE, Bellingham, WA, 2007), Vol. 6451, p. 64511M.

9. J. E. Rothenberg, D. F. Browning, and R. B. Wilcox, in *Third International Conference on Solid State Lasers for Application to Inertial Confinement Fusion*, edited by W. H. Lowdermilk (SPIE, Bellingham, WA, 1999), Vol. 3492, pp. 51–61.

10. "Simulations of the Propagation of Multiple-FM Smoothing by Spectral Dispersion on OMEGA EP," published in this volume.

11. O. Morice, Opt. Eng. **42**, 1530 (2003).